ACS APPLIED MATERIALS & INTERFACES

Research Article

www.acsami.org

Enhancing the Interface in Silk–Polypyrrole Composites through Chemical Modification of Silk Fibroin

Isabella S. Romero,[†] Morgan L. Schurr,[†] Jack V. Lally,[†] Mitchell Z. Kotlik,[‡] and Amanda R. Murphy*[,†]

[†]Department of Chemistry and [‡]Department of Engineering Technology, Western Washington University, 516 High Street, Bellingham, Washington 98225, United States

Supporting Information

ABSTRACT: To produce conductive, biocompatible, and mechanically robust materials for use in bioelectrical applications, we have developed a new strategy to selectively incorporate poly(pyrrole) (Ppy) into constructs made from silk fibroin. Here, we demonstrate that covalent attachment of negatively charged, hydrophilic sulfonic acid groups to the silk protein can selectively promote pyrrole absorption and polymerization within the modified films to form a conductive, interpenetrating network of Ppy and silk that is incapable of delamination. To further increase the conductivity and long-term stability of the Ppy network, a variety of small molecule sulfonic acid dopants were utilized and the properties of these silk-conducting polymer composites were monitored over time. The composites were evaluated using attenuated total reflectance Fourier transform infrared spectroscopy (ATR-FTIR), scanning electron microscopy (SEM), optical microscopy, energy-dispersive X-ray (EDX) spectroscopy, cyclic voltammetry, a 4-point resistivity probe and mechanical testing. In addition, the performance was evaluated following exposure to several biologically relevant enzymes. Using this strategy, we were able to produce mechanically robust polymer electrodes with stable electrochemical performance and sheet resistivities on the order of 1×10^2 Ω/sq (conductivity ~1 S/cm).

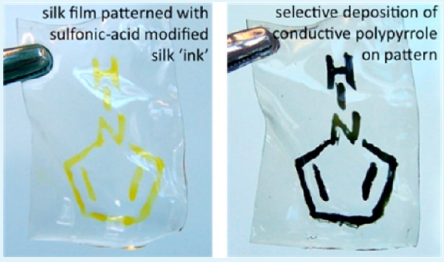

KEYWORDS: *silk, fibroin, Bombyx mori, conducting polymer, poly(pyrrole), electrodes*

1. INTRODUCTION

Materials capable of conducting electricity have numerous biomedical applications including use as electrodes for neurological stimulation and recording,[1,2] tissue engineering,[3] artificial muscles,[4] and stimuli-responsive actuators or sensors.[4] Pure metal or metal-backed electrodes have traditionally been used for bio-stimulation, but have significantly different mechanical properties than biological tissues, and can damage nearby biomolecules through adverse redox reactions that occur on the electrode surface.[1,2,5] These factors commonly result in inflammation and scar tissue encapsulation of metal electrodes, which drastically weakens signal transfer to and from the electrode.[1] Replacing metals with electrodes employing conducting polymers (CPs) is anticipated to alleviate several of these problems.[1,2,5] By varying the chemical structure, the mechanical properties of CPs can be tuned to match the properties of biological tissues,[6] thereby reducing inflammation and damage at the implant site. In addition, cells can adhere directly to the surface of CPs, which can increase the efficiency of electrical signal delivery/recording due to the intimate contact between cells and the electrode surface. Finally, CPs such as poly(pyrrole) (Ppy)[7−9] and poly(3,4-ethylenedioxythiophene)[10,11] lack significant in vivo toxicity making them appropriate materials for long-term implantation. To this end, our aim is to develop "soft", flexible, CP-based electrode materials that can be integrated into biological tissues with minimal damage to the host.

Although electrodes composed purely of CPs would be ideal, these polymers are typically brittle and insoluble, which precludes molding or processing of these materials into 3D electrode structures. Recent progress has been made to tailor the properties of conducting polymers by synthesizing copolymers containing flexible and conducting segments, but to date these copolymers suffer from either low conductivity or poor mechanical properties.[6,12−16] An alternative approach to enhancing the mechanical properties of CPs without reducing the conductivity has been to make layered composite materials by depositing CPs onto a secondary polymer that has superior mechanical properties. This strategy was first developed in the textile industry to confer anti-static or electromagnetic shielding properties to fabrics such as polyester and nylon,[17] and has recently been extended to the development of materials intended for biomedical applications. Several types of biodegradable synthetic polymers[9,18−21] and natural fibers[22−25] have been coated with CPs. These composites tend to have higher conductivity than the degradable copolymers discussed above. However, in general, a poor interfacial bond is formed when the CP is indiscriminately precipitated on the surface of the second polymer scaffold, which limits the long-term stability of the composites. For this approach to be feasible, the interfacial adhesion between the two materials must be

Received: August 31, 2012
Accepted: December 31, 2012
Published: January 15, 2013

strong in order to prevent delamination and subsequent failure of the device.

In this work, we report our efforts to employ the natural polypeptide silk fibroin as the platform material for conducting polymer composites. Silk is an attractive scaffold because of its excellent mechanical properties, biocompatibility, slow degradation profile, and aqueous processability.[26] It is inexpensive and readily available through direct isolation of the fibroin protein from *Bombyx mori* silkworm cocoons. The amino acid sequence of silk fibroin contains repetitive glycine-alanine-glycine-alanine-glycine-serine (GAGAGS) repeats, which can self-assemble into an anti-parallel β-sheet structure.[27] These β-sheets are highly crystalline and essentially crosslink the polymer through strong intra- and inter-molecular hydrogen bonds, giving the material high mechanical strength. Silk fibers can be dissolved in aqueous lithium bromide, and then dialyzed against water to give aqueous silk solutions that can be processed into films, fibers, hydrogels, and high-surface area 3D sponges.[26,28] Key to the work described here, silk has several amino acids that are available for chemical modification, allowing the chemical properties of the protein to be tuned.

Previous work has shown that polypyrrole will precipitate onto silk textiles,[29,30] and very recently, electrospun films made from regenerated silk.[31] Here, we describe an alternative strategy for selectively incorporating conductive Ppy into silk structures. This was achieved by first modifying the tyrosine side chains in the silk fibroin protein with sulfonic acid groups using a diazonium coupling reaction.[32] These acid-modified silk derivatives were found to promote the absorption and intercalation of positively charged Ppy into the negatively charged silk network, resulting in robust and selective adhesion between the platform silk material and the conducting polymer. This method allowed significantly lower pyrrole and $FeCl_3$ concentrations to be used than those previously reported for deposition of Ppy on unmodified silks.[29−31] It also dramatically increased the interfacial bond between silk and Ppy by forming an interpenetrating network of the two polymers, and enabled spatial control of conducting polymer deposition within a larger silk construct. The resulting composites were evaluated using attenuated total reflectance Fourier transform infrared spectroscopy (ATR-FTIR), scanning electron microscopy (SEM), optical microscopy, energy-dispersive X-ray (EDX) spectroscopy, cyclic voltammetry, 4-point resistivity probe and mechanical measurements. The stability of the materials when exposed to biologically-relevant enzymes was also monitored. Overall, we were able to produce biocompatible, stable, mechanically robust polymer electrodes with sheet resistivities on the order of 1×10^2 Ω/sq (conductivity ~1 S/cm).

2. MATERIALS AND METHODS

Materials and Instrumentation. All chemicals were purchased from Aldrich, Sigma or Fluka and used without further purification. Cocoons from the *Bombyx mori* silkworm were obtained from the Tissue Engineering Resource Center (TERC) at Tufts University. Infrared spectra were measured on solid films in ambient atmosphere with a Fourier transform infrared spectrometer (FTIR) (Thermo-Scientific Nicolet IS10) equipped with an attenuated total reflectance (ATR) accessory. Topography and cross sections of silk films were visualized by scanning electron microscopy (SEM) using a Vega TS 5136MM with an energy dispersive X-ray (EDX) spectrometer and retractable backscatter detector (BSE). Films were fractured in liquid nitrogen to visualize cross sections, and all samples were mounted with carbon tape on aluminum stubs. Samples coated with Ppy were conductive enough to be imaged directly, while all non-conductive samples were coated with gold prior to imaging with SEM. Optical microscopy was performed using an Olympus SZX16 Optical Microscope. A razor blade was used to obtain thin slices of film cross sections for imaging. Sheet resistivity measurements were made with a Lucas Labs S-304-2 4-point resistivity probe (Signatone SP4-40045TBY tip) powered by a Keithley 2400 Sourcemeter. Cyclic voltammetry experiments were carried out using a Pine Research Instrumentation WaveNow potentiostat, and data were recorded and analyzed using AfterMath software. Counter and reference electrodes were purchased from Bioanalytical Systems, Inc.

Preparation of Aqueous Silk Solutions. Aqueous silk solutions were obtained using previously published protocols with slight modifications.[32] Twelve cocoons from the *B. mori* silkworm were cut into pieces and rapidly boiled in an aqueous solution of 0.02 M Na_2CO_3 (3 L) for 1 h. The resulting fibers were rinsed once with boiling distilled (DI) water, three times with room temperature DI water, and then dried at room temperature. The purified silk fibers were dissolved in a solution of 9 M LiBr at 60°C for ~1 h to make a 20% (w/v) silk solution. This solution was placed into a dialysis cassette (Pierce Slide-a-lyzer G2, 3.5k MWCO, 5-15 mL capacity), and dialyzed against 1 L DI water per dialysis cassette for three days, changing the water five times. The pH of the water was adjusted using HCl so that the final silk solution was pH 6-7. After removal, the resulting silk solution was filtered through a 5 μm pore size syringe filter. The final solution typically had a concentration of 7-8% (w/v), and was stored at 4 °C.

Silk solutions in borate buffer were also prepared following a similar protocol. Silk fibers were dissolved in LiBr as described above, and dialyzed against 1 L DI water for two days, changing the water three times. The silk solution was then dialyzed against 1 L borate buffer (100 mM borate, 150 mM NaCl, pH 9) for an additional day, changing the buffer once. The solution was removed and stored at 4 °C.

Preparation of Insoluble Silk Films. To prepare solid silk films, we pipetted 100 μL aliquots of aqueous silk solution onto polystyrene Petri dishes (non-tissue culture treated), dried overnight, then soaked in 70% ethanol overnight. Since films were cast free-form, slight variations were seen in the diameter and thickness of the films. The next day, the films were rinsed thoroughly with DI water and stored in DI water. *Unmodified silk film.* ATR-FTIR: 1235, 1269, 1516, 1620 cm^{-1}.

Diazonium Coupling on the Surface of Insoluble Silk Films. Previously reported methods for diazonium coupling reactions with silk[32] were adapted for modification of pre-formed, solid silk samples. Insoluble silk films (typically twelve 9 mm films) were soaked in 8 mL of borate buffer (100 mM borate, 150 mM NaCl, pH 9) on ice for 30 min prior to reaction. The diazonium salt of sulfanilic acid was prepared by dissolving 34 mg (0.2 mmol) sulfanilic acid and 152 mg (0.8 mmol) *p*-toluene sulfonic acid monohydrate in DI water (2 mL). Once dissolved and cooled on ice, 34 μL of 4 M $NaNO_2$ was added to the solution and left to react on ice for 15 min. The diazonium salt solution (2 mL) was then added to the films in borate buffer, and was allowed to react for 40 min on ice. The resulting acid-modified films were rinsed 4-5 times with DI water and stored in DI water at room temperature. *Acid-modified silk.* ATR-FTIR: 1007, 1032, 1122, 1234, 1521, 1620 cm^{-1}.

Poly(pyrrole) (Ppy) Deposition on Silk Films. *General Procedure.* To deposit Ppy on plain or acid-modified silk films (prepared as described above), films were submerged in an aqueous solution containing 50 mM pyrrole. To initiate polymerization, anhydrous $FeCl_3$ (7.5 mM final concentration) was added and the solution was left to react for 30 min to 4 h at room temperature. Optimal polymerization time was found to be 2−3 h. Films were rinsed thoroughly with DI water and stored in DI water at room temperature. The effects of increasing $FeCl_3$ ratio were also studied. For these samples, the concentrations of 7.5, 11, and 15 mM $FeCl_3$ were compared. *Plain film with Ppy.* ATR-FTIR: 1235, 1520, 1620 cm^{-1}. *Acid-modified surface with Ppy.* ATR-FTIR: 1030, 1160, 1319, 1516, 1619 cm^{-1}.

Doped Samples. To increase conductivity of the Ppy coatings, some samples also contained small molecule anionic dopants that were incorporated into the films during pyrrole polymerization. Dopants were added at the start of the polymerization reaction at a concentration of 0.1 molar equivalent of the dopant relative to pyrrole. Dopants tested included *p*-toluenesulfonic acid (*p*-TSA), a combination of anthraquinone-2-sulfonic acid (ASA) and 5-sulfosalicylic acid (SSA) in a 1:4 ratio of ASA to SSA,[33] and (−)-camphor-10-sulfonic acid (CSA). In addition, the use of poly(styrene sulfonate) (MW 70k) as a dopant was evaluated at a concentration of 0.1 molar equivalent of *sulfonic acid groups* relative to pyrrole.

Patterned Silk Films. Patterned silk films were made by first preparing aqueous acid-modified silk 'inks' in the following manner. The diazonium salt of sulfanilic acid was prepared as described above. The resulting diazonium salt solution (2 mL) was added to 8 mL of the silk solution in borate buffer (~8 wt %), vortexed briefly, and then left to react on ice for 20 min. The resulting solution was loaded into a dialysis cassette (Pierce Slide-a-lyzer G2, 3500k MWCO, 5−15 mL capacity), and dialyzed against DI water (1 L) for three days, changing the water four times. The resulting solutions (~2−3 wt %) were concentrated by dialyzing against a 10 wt % poly(ethylene glycol) (PEG) solution for up to 24 h, resulting in aqueous silk "inks" containing 14−19 wt % acid-modified silk.

Surface adhered silk films were prepared by pipetting aqueous solutions of plain silk (100 μL) into tissue culture treated 6-well plates. The solutions were air-dried overnight to form a film, treated with 70% ethanol for 24 h, and then rinsed with DI water (films stayed adhered to the well surface throughout). Free-standing silk films were also prepared by casting 8 mL of an 8 wt % aqueous silk solution into a 76 x 127 mm single well polystyrene plate, followed by drying overnight. These films were thick enough to be removed from the plate, cut into the desired size, soaked in 70% ethanol for 24 h, and then rinsed with DI water. Acid-modified 'inks' prepared as described above were then stamped or painted onto the plain silk films, air-dried overnight, then treated with pure methanol to induce crystallization of the patterned silk and render it insoluble. Aqueous mixtures of alcohols (such as the 70% ethanol used to crystallize plain silk films) were found to be insufficient for crystallizing the acid-modified silk, and resulted in partial dissolution of the patterns. Ppy was deposited on the patterned films using the methods described above where the films were soaked in 50 mM pyrrole and 7.5 mM $FeCl_3$ for 2 h.

Adhesion Test of Ppy Coatings. A modified version of "Measuring Adhesion by Tape Test" (ASTM D3359) was used. A piece of Scotch brand invisible tape was placed firmly on the deposited polymer film and pressed gently to achieve even contact between tape and film, then gently peeled off. The visible quantity of Ppy removed by the tape from the surface of the silk film was used to compare the relative adhesion of the samples.

Electrical Characterization. Sheet resistivity of silk-conducting polymer films was measured in ambient atmosphere with a Lucas Labs S-304-2 four-point resistivity probe (Signatone SP4-40045TBY tip) powered by a Keithley 2400 Sourcemeter. Sheet resistivity was calculated based on current-voltage relationships in the films using the equation $R_s = 4.532(V/I)$, where V (volts) is the voltage measured across the two inner electrodes, I (amperes) is the current passed between the two outer electrodes, and R_s (Ω/square) is the sheet resistivity. The thickness of the polymer coatings was obtained by evaluating film cross sections with a light microscope or SEM. The thickness (cm) was then used to calculate the conductivity, σ (Siemens/cm), for a given film using the equation $\sigma = 1/(R_s t)$.

Electrochemical Characterization. Cyclic voltammetry (CV) was carried out using a 3-electrode cell equipped with a platinum wire counter electrode, and a Ag/AgCl reference electrode. Silk films (11.5 mm diameter circles) coated with Ppy served as the working electrodes. Contact was made to the films using copper tape that was encapsulated in Kapton tape to allow the film to be completely submerged in the electrolyte. The area of film exposed to electrolyte was 52 mm^2. Aqueous solutions containing 10 mM ASA/SSA (1:4 ratio) or 1 M phosphate buffered saline (PBS) were used as the supporting electrolyte. The ASA/SSA electrolyte does have redox activity in this window, however only microamperes of current were observed at the 10 mM concentration (see the Supporting Information), which was insignificant compared to the current flow through the silk films. Scans were initiated at 0 V and swept through various ranges between −1.5 and +1.5 V at 15−100 mV/s. Decreases in charge storage capacity over time were calculated by comparing the area of the voltammagrams at different time points.[34]

Mechanical Testing. To test the tensile properties of silk films before and after Ppy deposition, the "Standard Test Method for Tensile Properties of Thin Plastic Sheeting" (ASTM D882) was used. Samples were prepared by casting 8 mL of an 8 wt % aqueous silk solution into a 76 × 127 mm single well plate. Films were dried, treated with 70% ethanol overnight, then cut into 13 × 76 mm strips. Sample thicknesses were between 40 and 100 μm, as measured using calipers and further verified by measuring the cross section using SEM. Ten of these strips were left as is (plain silk films), 20 were acid-modified as described above, and 20 were subjected to acid-modification followed by Ppy deposition. Therefore, the mechanical properties given are the average from 10 or more samples. Samples were tested on an MTS Sintech frame using a 25 lbf capacity force transducer (MTS #100-090-900), which was first calibrated by testing cellophane samples with known tensile properties (Innovia P25-400). During testing, rectangular pieces of cellophane were cut and sandwiched on each side of the silk film to prevent the grips from damaging the soft films. These materials are intended for use in biological fluids, so samples were hydrated prior to testing since the mechanical properties of silk change in the dry versus hydrated state.[35,36] Silk films were soaked in DI water for at least 24 h, blotted dry, and then tested immediately at ambient temperature and humidity. The ultimate tensile strength, Young's modulus and the % elongation at break were measured.

Enzymatic Degradation of Silk Films. Three types of insoluble silk films were evaluated: (1) plain silk films, (2) acid-modified films, and (3) acid-modified films with a Ppy coating doped with ASA/SSA (all prepared as described above). Films were dried, weighed, and placed in individual wells of a 24-well plate. Enzyme solutions were prepared by dissolving protease XIV from *Streptomyces griseus* (Sigma P5147, specific activity 7.3 U/mg), collagenase type IA (Sigma C9891, specific activity 821.5 U/mg), or α-chymotrypsin (Sigma C4129, specific activity 57.2 U/mg) in 5 mM solutions of Ca^{2+} in nanopure water (pH 7.0) to give final solutions with concentrations of 10 enzyme units (U)/mL. Dry films were immersed in the protease solutions, then incubated at 37 °C and removed after 1, 3, 5, and 10 days (three films of each type were evaluated under each condition). The enzyme solutions were replaced daily with fresh solutions. Silk films in 5 mM Ca^{2+} in nanopure water (pH 7.0), as well as films exposed to 1 mg/mL bovine serum albumin were used as controls. Upon removal, silk films were rinsed thoroughly, and then soaked in DI water for two days before characterization. Films were dried completely and weighed. The change in mass was used to calculate percentage weight loss. The sheet resistivity and the electrochemistry of the silk-Ppy composite films were probed before and after enzyme degradation. For CV studies, electrical contact was made to the films prior to soaking in the enzyme solution as described in the CV section. All data reported are the average of three individual films treated in an identical manner.

3. RESULTS AND DISCUSSION

3.1. Diazonium Coupling Reaction. To covalently install sulfonic acid groups on the silk protein, we used a diazonium coupling reaction that occurred via electrophilic aromatic substitution between silk tyrosine residues and the diazonium salt of sulfanilic acid (Scheme 1).[32] Although the majority of the silk protein is composed of non-reactive amino acids, approximately 5% of the amino acid composition is tyrosine, allowing incorporation of up to ~280 sulfonic acid groups per protein.[27] We had previously established that the diazonium

Scheme 1. Diazonium Coupling Reaction Used to Synthesize "Acid-Modified Silk"

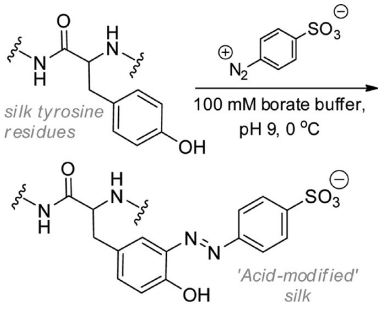

coupling reaction could be performed on silk solutions dissolved in buffer,[32] and that technique was extended here to modify the surface of insoluble silk films. The reaction was monitored visually where a distinct change from colorless to orange was observed within minutes upon addition of the diazonium salt (Figure 1a). This color change was indicative of

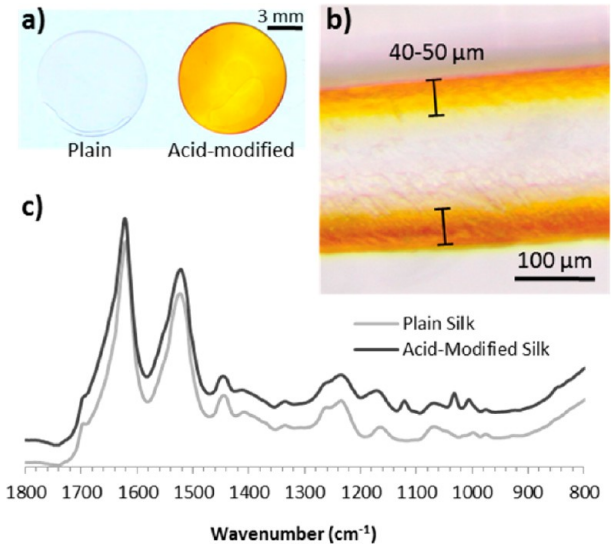

Figure 1. (a) Photograph of a plain and an acid-modified silk film. (b) Optical microscope image of the cross section of an acid-modified silk film. (c) ATR-FTIR spectra (*y*-axis shows absorbance) of a plain and an acid-modified silk film. Spectra were normalized to the silk C═O vibration at 1625 cm^{-1} and offset for clarity.

the formation of the azo bond between the tyrosine residues and the diazonium salt, and was used to track the approximate depth of penetration into solid silk films. As shown in Figure 1b, cross sectional images revealed orange/yellow bands on both sides of the films that extended approximately 40−50 μm into the surface. Therefore, for films with a total thickness greater than ∼100 μm, a clear band of unmodified silk was observed in the center of the films.

The diazonium reaction was further characterized using ATR-FTIR and EDX. Small, but discernable peaks corresponding to the S−O and S═O vibrations appeared in the ATR-FTIR spectra at 1007, 1032, and 1122 cm^{-1} in the acid-modified samples (Figure 1c). EDX analysis also confirmed the presence of sulfur in all of the acid-modified samples (see the Supporting Information). An equal atomic percent of sodium to sulfur was also found in the acid-modified films, where sodium is presumably serving as a counterion to the deprotonted sulfonic acid groups.

3.2. Deposition of Undoped Poly(pyrrole) on Silk Films. Because of the intractability of preformed polymers of pyrrole, Ppy must be deposited on silk constructs in situ during the polymerization of pyrrole. Chemical polymerization of pyrrole occurs in the presence of oxidizing agents such as $FeCl_3$ through the coupling of radical cation intermediates. The resulting polymer assumes an oxidized, cationic state.[37] As discussed in the Introduction, using this in situ deposition method to coat natural and synthetic polymers usually results in Ppy particles randomly precipitating from solution onto the polymer surface. Here, we demonstrate that chemical modification of the silk surface to introduce negatively charged, hydrophilic sulfonic acid groups can selectively promote pyrrole absorption and polymerization within acid-modified silk films to form a conductive, interpenetrating network of the cationic Ppy and the anionic silk.

In our initial studies, plain (unmodified) and acid-modified silk films were exposed to 50 mM pyrrole and 7.5 mM $FeCl_3$ in water for 30 min, 1 h, 2 h, and 4 h at room temperature. As shown in Figure 2a, opaque glossy black coatings of Ppy formed on the acid-modified silks after 1 h of reaction, while plain silk films only began to show significant color at the 4 h time point. Ppy deposition was further confirmed using ATR-FTIR, where new absorptions corresponding to Ppy appeared at 965, 1030, 1160, and 1290 cm^{-1} in the acid-modified silks (Figure 2b). No peaks for Ppy were observed on the plain silk films exposed to the same polymerization conditions (Figure 2b). For the plain films, only the 4 h time point samples had measurable sheet resistivities of 6.4 ± 1.8 × 10^5 Ω/sq. In contrast, the sheet resistivity of acid modified films dramatically decreased from 1.1 ± 0.4 × 10^6 Ω/sq to 5.3 ± 1.0 × 10^3 Ω/sq between 30 min and 2 h, but only decreased slightly between 2 and 4 h to reach 1.7 ± 0.3 × 10^3 Ω/sq (conductivity ∼0.1 S/cm).

The Ppy coating on the plain silk after 4 h was very thin, transparent, and easily flaked from the surface during handling, while all Ppy coatings on the acid-modified silks were robustly adhered. No flaking or delamination of the Ppy coatings was observed after repeated bending, washing or scraping of the acid-modified films. To further verify adhesion, a 'Scotch tape test' was performed where a piece of Scotch brand invisible tape was firmly placed on silk films coated with Ppy, and then was carefully peeled off. In each trial with the acid-modified silk substrates, only a slight grey haze was removed with the tape (Figure 2c), leaving the conductive black Ppy layer intact. The small amount of Ppy that did deposit on the plain silk films at long polymerization times was easily removed, so grey smudges were also observed on the tape after removal from the plain silk films (Figure 2c).

Before further discussion of the film morphologies, it should be noted that differences were consistently observed between the two sides of the silk films. To form the films, aqueous silk solutions were deposited, dried, and crystallized on a Petri dish. The "Petri dish" side of the film was consistently smoother because the silk was confined to the smooth surface of the Petri dish during drying and crystallization. Ppy coatings deposited on the side of the films that dried in contact with the Petri dish were typically thinner and more resistive than the coatings on the sides of the silk films that dried facing the air. The difference between the two sides was less pronounced when films were cast on rougher or more hydrophilic surfaces.

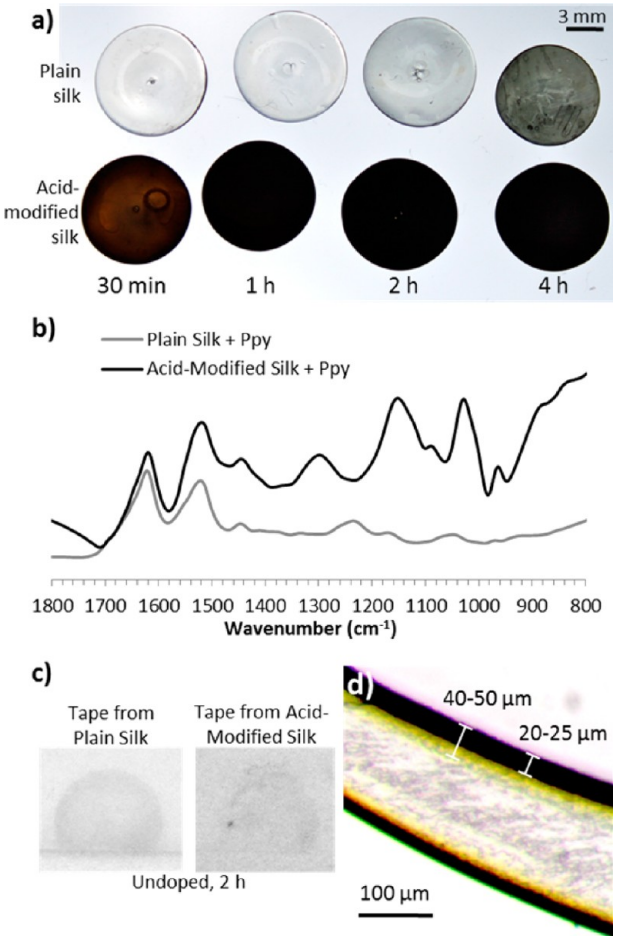

Figure 2. (a) Photographs of plain and acid-modified silk films exposed to 50 mM pyrrole and 7.5 mM $FeCl_3$ in water for the times given. (b) ATR-FTIR spectra (*y*-axis shows absorbance) of plain and acid-modified silk after Ppy deposition for 2 h. Spectra were normalized to the silk C═O vibration at 1625 cm^{-1} and offset for clarity. (c) Photographs of the Scotch tape that was adhered and then removed from plain and acid-modified silk-Ppy films exposed to the pyrrole polymerization mixture for 2 h. (d) Optical microscope image of the cross section of an acid-modified silk film after Ppy deposition for 2 h. The depth of sulfonic acid and Ppy penetration are highlighted.

Therefore, we suspect that inhibition of Ppy absorption leading to higher sheet resistivity is likely due to decreased porosity on the side of the film dried on the smooth Petri dish surface. Further explanation may lie in the SEM images of the film cross sections (see Figures 3, 4, and 6). Vertical striations indicative

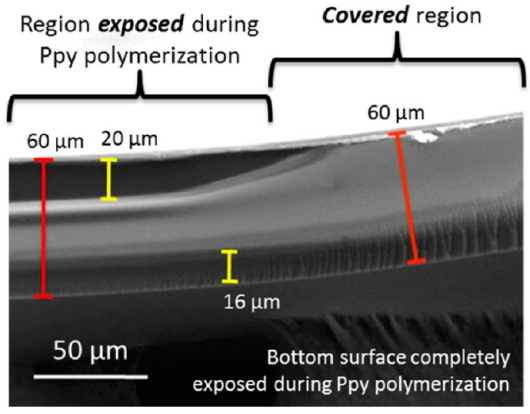

Figure 4. SEM image showing the cross section of an acid-modified silk film where a portion of the film was covered with tape during a 2 h exposure to the pyrrole polymerization mixture. The thickness of the black Ppy layer (yellow), as well as the thickness of the entire film (red) in the covered and exposed regions are indicated.

of a crystalline lamellae structure were commonly seen on the side of the silk film that dried in contact with the Petri dish surface, suggesting that the surface induced order on the silk protein. The difference in crystallinity of the silk protein on either side of the film could also explain the differences in Ppy deposition. Although the properties varied on the side of the films that dried touching the Petri dish surface, the side of the films that dried towards the air produced very consistent results independent of the surface on which it was cast. Therefore, for clarity, all results presented in the remainder of this manuscript will focus on the side of the silk films that dried in contact with air. Further study of the differences between the two sides of the silk films is the subject of ongoing investigations and will be reported in due course.

Although the non-conductive plain and acid-modified silk films required sputter-coating with gold prior to SEM imaging,

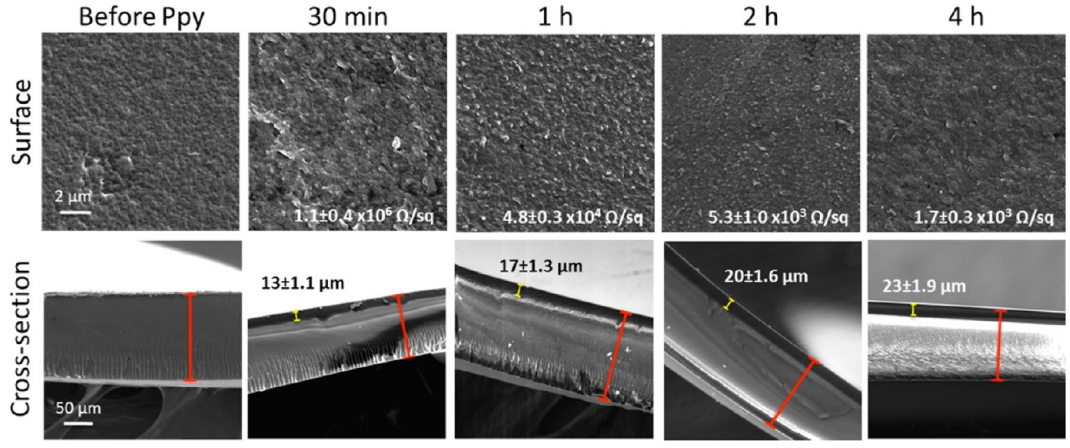

Figure 3. SEM images of the surfaces and cross sections of acid-modified silk films before and after exposure to 50 mM pyrrole and 7.5 mM $FeCl_3$ in water for the times given. In the cross sectional images, the thickness of the black Ppy layer on the side of the film that dried towards the air (yellow), as well as the thickness of the entire film (red) are highlighted.

dx.doi.org/10.1021/am301844c | ACS Appl. Mater. Interfaces 2013, 5, 553−564

the acid-modified films coated with Ppy were conductive enough to be directly imaged. Surprisingly, the images of the pristine surfaces revealed that the Ppy coatings exhibited morphologies nearly identical to the underlying acid-modified silk film. As shown in Figure 3, the sides of the acid-modified silk films that dried towards the air had smooth nodular morphologies, which did not change significantly after deposition of the Ppy. Retention of the initial silk morphology and lack of clear Ppy particle precipitation as typically seen on the surface of Ppy coated polymers suggested that the pyrrole polymerization was either templated by the silk surface or was occurring below the surface of the acid-modified silk films.

To further investigate how the Ppy was adhering to the acid-modified silk, we fractured films in liquid nitrogen and imaged the cross sections using SEM. Again, no metal coatings were deposited on the samples containing Ppy prior to imaging. Although the surfaces of the films containing Ppy were sufficiently conductive to image without a metal coating, the cross sections expose an insulating silk layer in the center. This insulating band led to some charging and image distortion. However, trends were still clearly discernable in the images shown in Figure 3. New black bands were evident on both sides of the films in samples exposed to the pyrrole polymerization mixture, and as discussed above, were typically thicker on the side of the film that originally dried to air. After 30 min of exposure to the pyrrole polymerization mixture, a 13 ± 1.1 μm black region was clearly visible. From 30 min to 4 h, this black band slowly increased to 23 ± 1.9 μm, although variations in thickness between samples as well as variations within a single film made the differences between the 1, 2, and 4 h samples insignificant.

Upon further inspection, the black Ppy regions appeared to be sunken into the silk films rather than deposited on top of the silk. The vertical striations seen in the films as a consequence of the fracturing process propagated unchanged into the black Ppy regions, suggesting that the two materials were tightly integrated. In addition, no indication of delamination between the layers had ever been observed. To further probe this hypothesis, experiments were carried out in which portions of acid-modified silk films were covered with tape during the polymerization reaction. As shown in Figure 4, the overall thickness of the films did not change in the regions exposed to the polymerization mixture, yet a black band of similar thickness to previous experiments was found to extend down into the surface of the films. Although a thin layer of Ppy could be forming on the surface, the lack of a clear step height between the covered and exposed regions suggests that the amount of Ppy on the surface is insignificant compared to the amount absorbed within the film. Additional support for this theory was gained by careful examination of optical microscope images of thin slices of the film cross sections. Figure 2d shows a cross section of an acid-modified film exposed to the polymerization mixture for 2 h. Here again, the overall film thickness does not change significantly following Ppy deposition, and black bands of similar thickness to that observed in SEM are seen on both sides of the film. The thickness of the acid-modification layer before Ppy deposition was ~40-50 μm, but after deposition only ~20 μm of the yellow/orange band is still visible suggesting that the other ~20 μm is obscured by the Ppy. These observations all corroborate our hypothesis that the Ppy sank into the film, as opposed to forming a distinct layer on top of the silk.

Using the initial reaction conditions, the depth of Ppy penetration seemed to be limited to ~25 μm. To investigate whether the reaction conditions could be varied to encourage deeper deposition, we soaked films in 50 mM pyrrole overnight before addition of 7.5 mM $FeCl_3$, or soaked them in $FeCl_3$ overnight prior to pyrrole addition. No change was seen in the Ppy deposition depth in either case, indicating that time is not the limiting factor for diffusion of one or both of the reactants into the films. Rather, rapid polymerization and a resulting increase in polymer density at the surface likely limits diffusion of both the pyrrole and $FeCl_3$ into the interior of the films.

The collective observations that (1) the Ppy was robustly adhered to the acid-modified silk, (2) the surface morphology did not significantly change after Ppy deposition, (3) a step height was not observable in patterned films, and (4) the thickness of the Pyr band does not significantly increase with extended reaction time all suggest that the Ppy formed an interpenetrating network within the silk, rather than a distinct two-layer composite. In previous work it has been shown that sulfonic acid-modification significantly increases the hydrophilicity of silk.[32] Here, increased hydrophilicity as well as a strong affinity of the growing cationic Ppy for the anionic silk is likely responsible for facilitating absorption and retention of the Ppy. Although the depth of Ppy penetration did not significantly change with increased reaction time, the continued decrease in surface resistivity implies that the density or length of the Ppy chains does increase with time. The marked drop from 1×10^6 Ω/sq to 1×10^4 Ω/sq between 30 min and 1 h suggested that there was a percolation threshold that must be reached in order for the Ppy chains to have a continuous path for electron flow. The fact that the resistivity levels off after 2 h can be attributed to the limit in Ppy conductivity attainable using the given reaction conditions, as well as restricted diffusion of the monomer/oxidant into the dense Ppy/silk network.

3.3. Selective Deposition of Poly(pyrrole) on Acid-Modified Silk Patterns. The strong preference for Ppy intercalation with acid-modified silk was further exploited to obtain selective Ppy deposition on patterned silk films. As previously reported, the acid-modification reaction can be performed on silk dissolved in water.[32] Here, these acid-modified silk solutions were concentrated to 14−19 wt % and used as 'inks'. Plain silk films were patterned by painting or stamping acid-modified silk "inks" onto the surface. Patterned films were dried overnight, and then treated with pure methanol for 2 h to crystallize the acid-modified patterns and render them insoluble in water. When these patterned films were exposed to the pyrrole/$FeCl_3$ mixture, excellent selectivity for Ppy deposition on the acid-patterned regions was found for reaction times up to 3 h (Figure 5). At longer reaction times, Ppy began to precipitate across the entire film surface, but the majority of the precipitate could be easily wiped away from the unpatterned regions of the film, whereas the Ppy on the acid-modified patterns stayed robustly adhered. In Figure 5c, the 4 and 5 h wells were partially cleaned with a cotton swab (left side) to demonstrate this property.

3.4. Mechanical Testing of Modified Films. To determine whether our chemical modification sequence was affecting the mechanical properties of the silk, we measured the ultimate tensile strength (highest load recorded), Young's modulus, and % elongation at break for plain silk films, acid-modified films and acid-modified silks with Ppy. To make samples for tensile testing, 76 × 127 mm silk films were cast

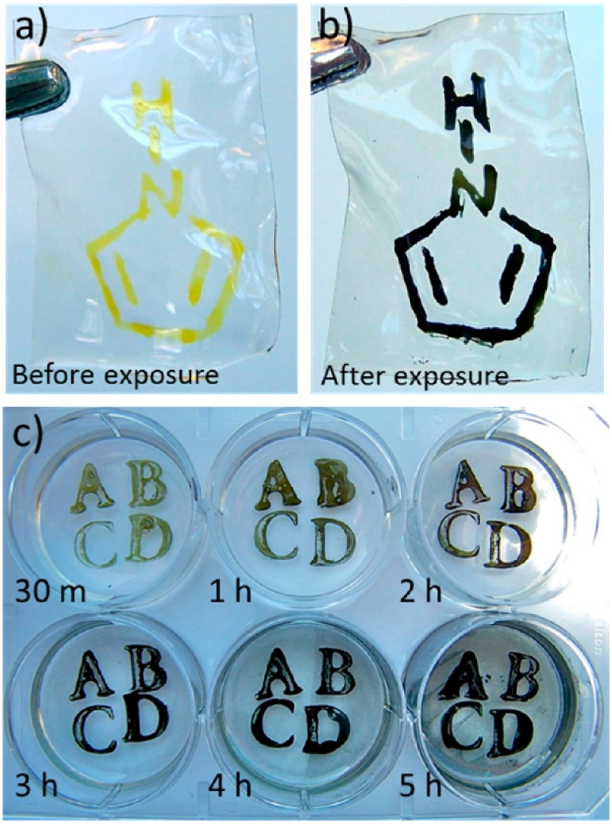

Figure 5. (a) Free-standing silk film painted with acid-modified silk "ink". (b) Film from (a) after exposure to 50 mM pyrrole and 7.5 mM $FeCl_3$ in water for 2 h. (c) Photograph of a well plate coated with plain silk films, stamped with acid-modified silk letters, and then exposed to pyrrole and $FeCl_3$ in water for the times given.

(average thickness ~60 μm), cut into 13 × 76 mm strips, and then chemically modified using conditions described above. A summary of the data is given in Table 1, and representative stress–strain curves are given in the Supporting Information.

Table 1. Mechanical Properties of Silk Films before and after Chemical Modification

sample	ultimate tensile strength (MPa)	Young's modulus (MPa)	% elongation at break
plain silk	5.3 ± 1.0	90.0 ± 17.4	17.4 ± 3.0
acid-modified silk	6.9 ± 1.8	115.1 ± 34.3	22.7 ± 6.6
acid-modified silk + Ppy	9.3 ± 1.8	232.6 ± 60.4	15.4 ± 5.6

The tensile and modulus values for the plain silk films were on par with previously reported values for silk films in a hydrated state.[35,36] The acid treated samples showed significant increases ($p < 0.01$) in the tensile strength as compared to the plain silk samples, giving an average peak tensile strength of 6.9 MPa (30% increase). Acid-modification also resulted in increased modulus and % elongation, but the increase was less significant ($p < 0.06$). The tensile strength and modulus increased even further when Ppy was incorporated into the surface, giving an average peak tensile strength of 9.3 MPa (75% increase compared to plain silk) and an average modulus of 232.6 MPa (158% increase compared to plain silk) (both $p < 1 \times 10^{-6}$). This modulus value was similar to that reported for free-standing Ppy films,[38] indicating that the interpenetrating Ppy layer was significantly contributing to the overall mechanical properties of the composite. It should also be noted that no delamination or flaking of the Ppy was observed during stretching, consistent with our conclusion that the Ppy is physically integrated within the silk structure.

3.5. Doping Effects on the Conductivity and Stability of the Ppy Coatings on Acid-Modified Silk. As demonstrated above, sheet resistivities on the order of 1×10^3 Ω/sq were obtained for composites containing silk modified with sulfonic acid groups and Ppy. While these values were on par with other biomaterials coated with Ppy,[9,18−21] we sought to increase the conductivity further by optimizing the synthesis and doping levels within the Ppy layer.

Increasing the amount of oxidant has been shown in the literature to increase the rate of pyrrole polymerization and conductivity of the resulting Ppy to a point, however excess oxidant can also over-oxidize and degrade the Ppy.[39,40] In our materials, rapid bulk polymerization in solution leading to precipitation of Ppy particles is not desired, so a balance must be struck that maximizes both the conductivity and the absorption of Ppy into the silk surface.[41] Increasing the amount of $FeCl_3$ from 0.15 to 0.33 molar equivalents of $FeCl_3$ relative to pyrrole lowered the sheet resistivity of the resulting composites by an order of magnitude to $8 \pm 3 \times 10^2$ Ω/sq. However, further increases in $FeCl_3$ concentration resulted in an undesirable amount of Ppy precipitation from solution onto the surface of the films. EDX analysis of these materials indicated a significant increase in chlorine retained from the $FeCl_3$. Chlorine was undetectable in the samples with the lowest oxidant loading (0.15 equiv), but was found at levels of 0.23 atomic percent for samples with the higher $FeCl_3$ loading (0.33 equiv). Importantly, although higher catalyst loadings lowered the initial sheet resistivity, the effect was transient and these materials rapidly became more resistive upon prolonged storage in water (Figure 7).

Therefore, more robust synthetic methods were sought that would result in composites with stable conductivity. Although initially concerned that the addition of organic dopants would inhibit absorption of the Ppy into the acid-modified silk films, we decided to evaluate the effect of adding sulfonic acid derivatives during the pyrrole polymerization reaction. Several molecules were screened including: a combination of anthraquinone-2-sulfonic acid (ASA) and 5-sulfosalicylic acid (SSA) (in a 1:4 ratio of ASA:SSA),[33] *p*-toluenesulfonic acid (*p*-TSA), (−)-camphor-10-sulfonic acid (CSA), and poly(styrene sulfonate) (PSS). The larger size and hydrophobicity of these dopant molecules, as compared to chloride ion, has been shown to improve Ppy organization and film quality and result in polymers with more stable properties.[42,43]

Each dopant (0.1 molar equivalent of sulfonic acid relative to pyrrole) was dissolved in water and added to the polymerization mixture containing pyrrole and $FeCl_3$ (0.33 equiv. relative to pyrrole), and left to react for 2 h. Studies using higher molar equivalents of the dopant did not result in increased conductivity; hence the smaller concentrations were used. In general, the addition of the small molecule dopants did not negatively impact the absorption of the Ppy films into the acid-modified silk. However, using ASA alone (no SSA) resulted in rapid bulk polymerization and precipitation of the Ppy, but no deposition on the silk. Attempts to use PSS as the dopant also failed. When PSS was added to the polymerization mixture, the Ppy preferentially formed in solution, likely

because of the high water solubility of the Ppy-PSS complex, and did not deposit in significant quantities on the silk.

The ASA/SSA combination, *p*-TSA and CSA were all effective at lowering the sheet resistivity of the silk-Ppy composites, giving values ranging from 4.0−4.8 × 10^2 Ω/sq (Fig. 6). The ASA/SSA doped samples consistently gave the best results, likely due to the favorable packing of these planar aromatic structures within the Ppy matrix,[42−44] and the ability of the SSA to prevent Fe^{3+} precipitation during the polymerization reaction possibly leading to higher molecular weight Ppy.[45] Analogous to the undoped films, the surfaces retained their smooth nodular morphologies after Ppy deposition (Figure 6). Likewise, Ppy deposition depth was similar to

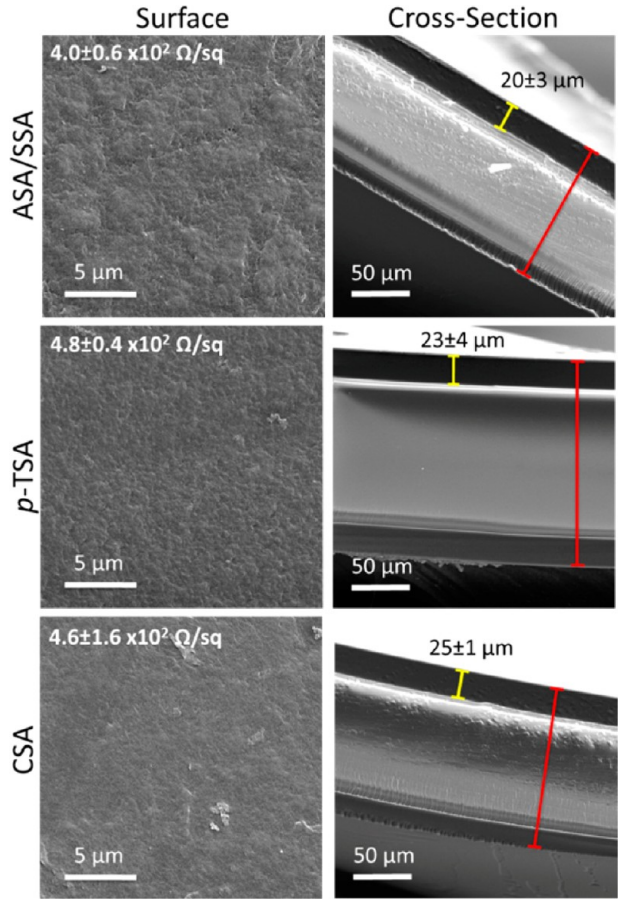

Figure 6. SEM images of the surfaces and cross sections of acid-modified silk films after deposition of Ppy doped with the small molecule sulfonic acids listed. The thickness of the black Ppy layer on the air-dried side (yellow), as well as the thickness of the entire film (red) are highlighted.

that of the undoped films, and differences in deposition between the dopants were statistically insignificant. The Ppy was found to penetrate ~20−25 μm into the silk surface, which corresponded to conductivities on the order of 1 S/cm.

The stability of doped films over time was further evaluated to determine if the Ppy coatings become more resistive over time due to degradation or dopant leaching. Samples were maintained in water for 28 days, and the resistivity was periodically evaluated. As shown in Figure 7, films containing ASA/SSA as the dopant were the most consistent, maintaining a low sheet resistivity of 5.6 ± 0.5 × 10^2 Ω/sq after 28 days. Doping of Ppy films with ASA has been reported to increase

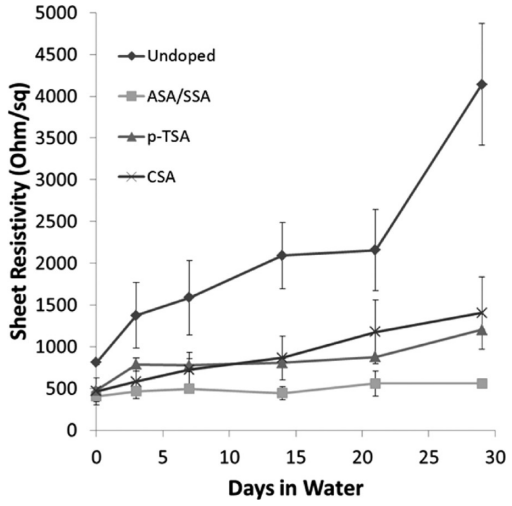

Figure 7. Plot of changes in sheet resistivity for acid-modified silk films with undoped and doped Ppy when stored in water for 28 days.

stability as a result of decreased oxygen penetration into the films because of the characteristically smooth morphology of Ppy-ASA films.[43] The resistivity of the *p*-TSA and CSA doped films were nearly identical to each other and steadily increased with time, but final values were only 2−3 times higher than the initial resistivities.

In addition to conductivity, the elemental compositions were evaluated over time using EDX (all data are listed in Supporting Information). Although quantification of light organic elements with EDX is difficult, clear trends between the samples were seen. For samples doped with ASA/SSA, a 60% increase in the sulfur content was initially seen as compared to the undoped samples, and this level of sulfur was maintained (within statistical error) throughout the 28 days. The *p*-TSA and CSA doped samples had a 20 and 10% increase, respectively, that both decayed slightly (but not significantly) over the 28 days. The increase in sulfur content indicated that the sulfonic-acid containing molecules are being absorbed and retained in the silk-Ppy composites, and likely serve as additional anionic dopants to stabilize the conductive cationic form of Ppy. The higher level of sulfur found in the ASA/SSA samples correlated with a higher observed conductivity, also suggesting that these molecules are serving as dopants. It was interesting to note that chlorine was undetectable in all of the doped samples, despite the higher catalyst loading, which is consistent with other reports that sulfonic acids are effective at displacing chlorine.[43]

From this data, we concluded that the incorporation of small molecule sulfonic acid dopants during polymerization was advantageous as it not only lowered the resistivity of the resulting composites, but it also increased their long-term stability. The combination of ASA/SSA had the best performance, and this was used for further studies detailed below.

3.6. Selectivity and Adhesion of Doped Ppy on Plain and Acid-Modified Silk. A consequence of doping the Ppy was that the deposition selectivity for acid-modified silk over plain silk was diminished, and significant darkening of plain silk films was observed. However, in all cases, the doped Ppy deposited on plain silk was 1−2 orders of magnitude more resistive than that of doped Ppy deposited on the acid-modified silk (Table 2). Imaging of the film surfaces and cross sections revealed that the Ppy coatings deposited on the plain silk films were very rough and easily flaked from the surface (see the

dx.doi.org/10.1021/am301844c | ACS Appl. Mater. Interfaces 2013, 5, 553−564

Table 2. Sheet Resistivity of Films Before and After Scotch Tape Adhesion Tests[a]

sample	dopant	initial sheet resistivity (Ω/sq)	sheet resistivity after tape removal (Ω/sq)
plain silk	none	1.5×10^5	7.6×10^5
acid-modified silk	none	1.5×10^3	2.3×10^3
plain silk	*p*-TSA	5.6×10^3	3.0×10^4
acid-modified silk	*p*-TSA	5.5×10^2	1.2×10^3
plain silk	ASA/SSA	1.6×10^4	1.2×10^5
acid-modified silk	ASA/SSA	5.4×10^2	7.8×10^2

[a]All films were synthesized ssing 0.33 equiv. of $FeCl_3$ relative to pyrrole.

Supporting Information). Therefore, the high resistivity of the Ppy on the plain silk could be attributed to the poor film organization and interconnectivity of the Ppy chains. Significant portions of the weakly adhered Ppy on plain films could be removed with Scotch tape. Photographs of the tape that was adhered and then removed from the various silk-Ppy films (not the films themselves) are shown in Figure 8. In all cases, the

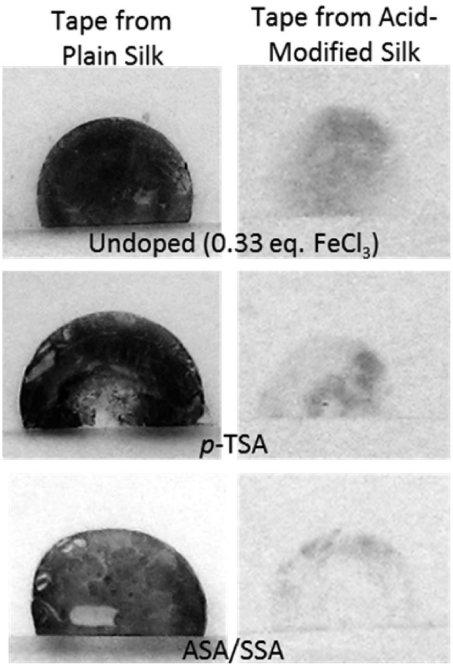

Figure 8. Photographs of the Scotch tape that was adhered and then removed from plain and acid-modified silk-Ppy films synthesized in the presence of the dopants listed. Doped Ppy films deposited on plain silk films are loosely adhered, and the majority of the film is removed with the tape as shown. In contrast, only a light grey haze was observed on the tape following removal from the acid-modified silk films, leaving the conductive Ppy layer intact.

majority of the Ppy deposited on plain silk becomes stuck to the tape and is easily removed, resulting in 5-7 fold increase in the sheet resistivities of the plain films (Table 2). In contrast, only light grey smudges were observed on the tape after removal from the doped Ppy films deposited on the acid-modified silk, which was likely from weakly adhered Ppy precipitates on the surface. The sheet resistivity of these samples rose only by 1.5−2 times after removal of the tape. Therefore, the addition of small molecule dopants to the polymerization mixture did not adversely affect the ability of the Ppy to penetrate into the acid-modified silk films, and composites with significantly higher conductivity than those formed with plain silk films were obtained.

3.7. Cyclic Voltammetry. Although the actual stimulation conditions for in vivo use will vary dramatically on the basis of the application,[1,2] preliminary electrochemical stability of ASA/SSA doped Ppy films was evaluated by subjecting the films to 200 oxidation and reduction cycles using cyclic voltammetry (CV). Studies were carried out in a 3-electrode cell equipped with a platinum wire counter electrode and an Ag/AgCl reference electrode. Circular acid-modified silk films (11.5 mm diameter) coated with Ppy containing the ASA/SSA dopant served as the working electrode. An aqueous solution containing 10 mM ASA/SSA (1:4 ratio) was used as the supporting electrolyte to minimize any effects of dopant exchange.

When films were cycled between −0.5 and +0.5 V, an oxidation peak at 0.3 V was observed, but no distinct reduction (Figure 9a). Surprisingly, when continuously cycled the films

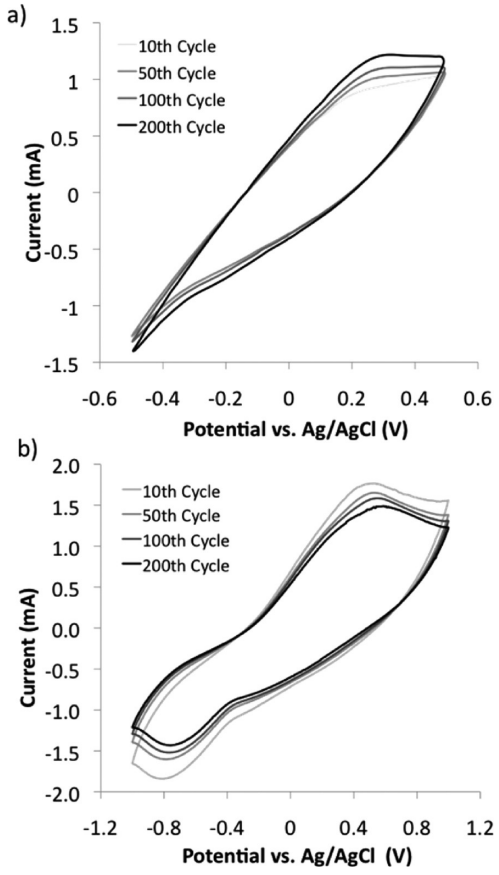

Figure 9. Cyclic voltammograms of an acid-modified silk film coated with ASA/SSA-doped Ppy. CV was performed (a) from −0.5 to +0.5 V at a scan rate of 15 mV/s or (b) from −1.0 to +1.0 V at a scan rate of 50 mV/s in an aqueous solution containing 10 mM ASA/SSA (1:4 ratio) using an Ag/AgCl reference electrode and a platinum wire counter electrode.

exhibited a 25% increase in charge storage capacity, as calculated by comparison of the area of the 10th scan and the 200th scan. To evaluate more extreme conditions, we repeated the experiment with a new film, cycling between −1.0 and +1.0 V.[46] In this broader window, films exhibited more distinct oxidation (~0.5 V) and reduction (−0.2 V and −0.8 V)

dx.doi.org/10.1021/am301844c | ACS Appl. Mater. Interfaces 2013, 5, 553−564

peaks (Figure 9b). While slight degradation was seen under these more aggressive conditions, films still retained 80% of their initial charge storage capacity from the 10th to the 200th scan. The majority of the current loss occurred during the first 50 oxidation and reduction cycles, suggesting that the film must be cycled for some time before a steady state electrolyte concentration in the film was reached.[47] A slight drift in the peak potentials was also observed, where the oxidation peak began at 0.49 V and shifted to 0.55 V after 200 cycles. Likewise, the major reduction potential shifted from -0.81 V to -0.73 V, and the smaller reduction peak shifted from −0.25 V to −0.24 V. Overall, these silk-supported Ppy films exhibited significantly higher stability as compared to literature reports of Ppy films deposited on platinum electrodes,[48,49] indicating their potential for use in long-term implants.

3.8. Enzymatic Degradation of Silk Films. As an initial simulation of how the silk-Ppy composites might perform upon in vivo use, films were exposed to several enzymes to mimic biodegradation. Films were exposed to solutions containing 10 units/mL collagenase, α-chymotrypsin, or a general protease (type XIV) that is known to degrade silk.[50] High enzyme concentrations were used to accelerate the degradation process, which would normally occur at a far slower rate. Three types of insoluble silk films (prepared as described above) were evaluated: (1) plain silk films, (2) acid-modified films, and (3) acid-modified films with a Ppy coating doped with ASA/SSA. Films were dried, weighed, immersed in the enzyme solutions, and then incubated at 37 °C for 1, 3, 5, or 10 days. Silk films soaked in 5 mM Ca^{2+} in nanopure water (pH 7.0) or in 1 mg/mL bovine serum albumin (BSA) were used as controls. Mass loss, surface resistivity, and electroactivity (measured with CV) of the films were evaluated over time.

As shown in Figure 10a, acid-modified and plain films exposed to protease XIV exhibited the largest degree of degradation as measured through mass loss. The acid-modified films disintegrated by 5 days, whereas the plain silk films still had a measurable mass until 10 days. The increase in degradation rate for the acid-modified films is likely due to the increased hydrophilicity as compared to the plain silk, which facilitated degradation and dissolution into the water. Coating the films with Ppy dramatically reduced the ability of the enzyme to degrade the silk protein resulting in only an 8% mass loss after 10 days. The same trend was observed when films were exposed to collagenase, although the total degradation was decreased as compared to protease XIV (Figure 10b). No significant mass loss (< 2%) occurred with the Ppy coated films, while the plain silk and acid-modified films lost 12 and 22% of their mass after 10 days, respectively. For films exposed to α-chymotrypsin, a 2−6% mass loss was observed after 10 days, but there was not a significant difference between each of the film types (see the Supporting Information). No mass loss was observed in films stored in water or in the presence of BSA.

Although slight variations in mass loss were observed upon exposure of the silk-Ppy composites to each of the enzymes, all films exhibited a uniform increase in sheet resistivity with time (Figure 11a). Resistivity rose roughly an order of magnitude at each time point, regardless of enzyme. The lack of correlation between extent of enzyme degradation and conductivity loss suggested that the effect was due to non-specific binding of the enzymes on the surface of the film,[7,51] rather than a specific degradation event. Films evaluated using SEM after exposure to the enzyme solutions had a significant amount of debris on the surface that charged heavily in the electron beam, suggesting that protein was accumulating on the surface. Furthermore, films soaked in solutions of BSA (a protein with no enzymatic activity) at comparable concentrations to the enzymes exhibited a similar, albeit smaller, increase in sheet resistivity over time.

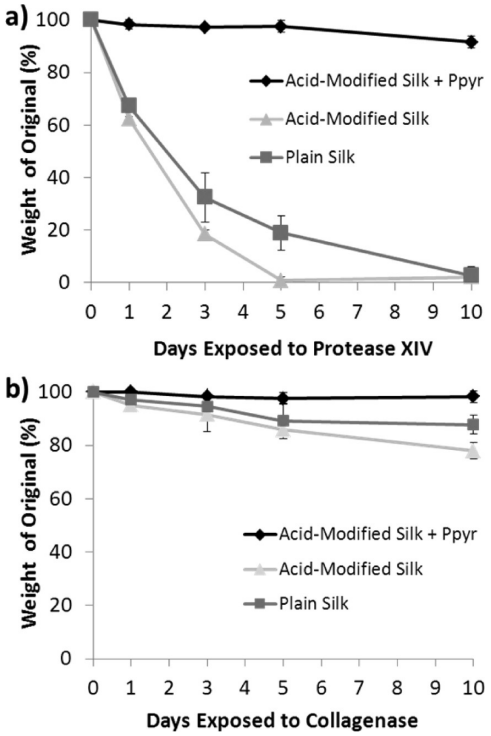

Figure 10. Mass loss of plain silk, acid-modified silk, and acid-modified silk with ASA/SSA doped Ppy exposed to 10 U/mL (a) protease XIV or (b) collagenase for 10 days.

To further evaluate the effects of enzyme exposure, we employed cyclic voltammetry to probe the electroactivity of the films over time. To avoid protein interference at the contact, we made electrical contact by adhering copper tape encapsulated in Kapton tape to one end of the films prior to enzyme exposure. As shown in Figure 11b, films did in fact retain their electroactivity throughout the 10 days of enzyme exposure. A shift in the reduction potential from −1.2 to −0.55 V and a ∼50% decrease in current were observed over time, suggesting some degradation. Again, the degradation could be due to decomposition of the Ppy backbone, or simply protein accumulation on the surface could be affecting the ability of ions to flow in and out of the films. Regardless of whether these changes are due to Ppy degradation or protein adsorption, the underlying Ppy films do retain a significant amount of electrical function as long as electrical contact is made to the film prior to biomolecule exposure.

The identity and conformation of proteins and other biomolecules that adsorb on the surface of materials exposed to biofluids can strongly dictate how cells will interact with the material. Several recent studies highlight the unique ability of conducting polymers to electrostatically control the conformation of biomolecules on their surface.[52−54] The ability of our silk-Ppy composites to attract biomolecules can therefore be used to our advantage, as it should be possible to tailor the composition and conformation of proteins on the surface by varying the oxidation state of the Ppy. Extension of our methods to the synthesis of 3D conductive silk scaffolds is also

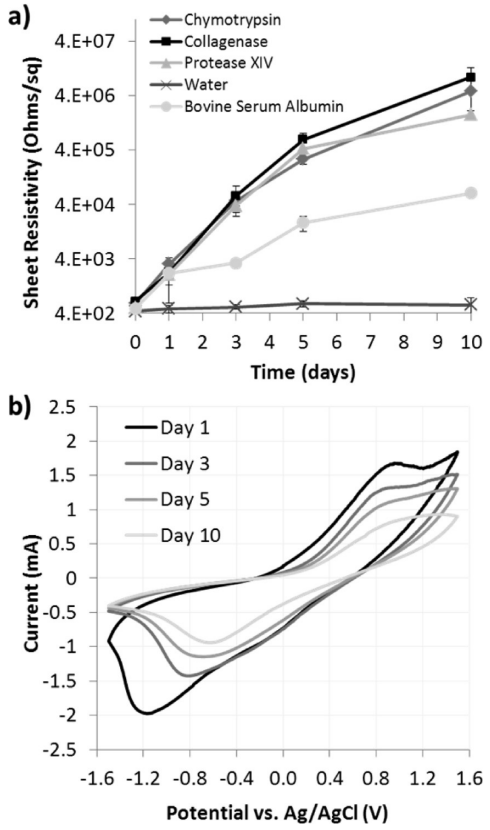

Figure 11. (a) Plot of sheet resistivity versus time for films exposed to 10 U/mL enzyme, 1 mg/mL BSA or water. (b) Cyclic voltammograms taken of the same film after exposure to protease XIV for the number of days given. CV was performed in an aqueous 10 mM ASA/SSA (1:4 ratio) solution at a scan rate of 25 mV/s using an Ag/AgCl reference electrode and a platinum wire counter electrode. The film was cycled twice at each time point, and the 2nd cycle is shown.

facile, leading to the possibility of spatial control of protein adsorption in three dimensions.

4. CONCLUSIONS AND OUTLOOK

Here we have described a strategy to produce a conductive interpenetrating network of silk fibroin and Ppy by augmenting the hydrophilicity of silk films through covalent attachment of sulfonic acid groups. Increased hydrophilicity of the silk surface as well as an electrostatic attraction between the two charged polymers drives the Ppy to completely intercalate within the silk during polymerization, resulting in the formation of robust composites that are incapable of delamination. We were able to produce mechanically strong silk-based electrodes with sheet resistivities on the order of 1×10^2 Ω/sq. These silk-Ppy electrodes also remained conductive after extended storage in water, and were stable towards repeated oxidation/reduction cycles. When exposed to proteases, the Ppy layer protected the silk from rapid degradation. Proteins were found to adsorb to the Ppy surface, but the underlying films retained their electroactivity. For ease of characterization, the majority of the optimization studies discussed here were for 2D films, but our findings can be directly translated into construction of conductive 3D silk structures that have a myriad of applications that will be discussed in forthcoming publications. We are currently using specially designed versions of these composites as electromechanical actuators,[4] with an eye towards developing implantable valves, drug delivery devices, or engineered tissues capable of controlled stimulation.

Crude patterning was also achieved by exploiting the selective adhesion of Ppy on our acid-modified silks versus plain silk. Refinement of our patterning techniques using soft lithography[55] or inkjet printing[56] will allow for the creation of complex microscale electrode patterns on the surface of our flexible, fully biocompatible silk films. Several future applications can be envisioned for these devices, including cell culture substrates capable of stimulating single cells or small groups of cells, spatial control of biomolecule adsorption on the surface,[52−54] or brain−computer interfaces placed on the surface of the brain to record brain activity.[57]

■ ASSOCIATED CONTENT

Supporting Information

CV of ASA/SSA solutions alone, EDX data, stress−strain curves of silk films before and after chemical modification, SEM and optical microscope images of plain silk films with doped Ppy coatings, and a plot of degradation vs time for films exposed to α-chymotrypsin. This material is available free of charge via the Internet at http://pubs.acs.org/.

■ AUTHOR INFORMATION

Corresponding Author

*E-mail: amanda.murphy@wwu.edu. Tel.: 1-360-650-3138.

Notes

The authors declare no competing financial interest.

■ ACKNOWLEDGMENTS

We are grateful for financial support from Western Washington University, M.J. Murdock Charitable Trust, a departmental development grant from the Research Corporation, as well as a grant to WWU's Advanced Materials Science and Engineering Center (AMSEC) from the M.J. Murdock Charitable Trust. We thank David Kaplan and the Tissue Engineering Resource Center (TERC) at Tufts University for resources for initial proof-of-concept experiments, and for providing silk cocoons. We thank Janelle Leger, David Rider, and John Antos for helpful discussions; Erin Macri for assistance with SEM; and Nicole Larson for help with mechanical testing.

■ REFERENCES

(1) Green, R. A.; Lovell, N. H.; Wallace, G. G.; Poole-Warren, L. A. *Biomaterials* **2008**, *29*, 3393−3399.
(2) Asplund, M.; Nyberg, T.; Inganas, O. *Polym. Chem. UK* **2010**, *1*, 1374−1391.
(3) Subramanian, A.; Krishnan, U. M.; Sethuraman, S. *J. Biomed. Sci.***2009**, *16* (108).
(4) Smela, E. *Adv. Mater.* **2003**, *15*, 481−494.
(5) Ateh, D. D.; Navsaria, H. A.; Vadgama, P. *J. R. Soc. Interface* **2006**, *3*, 741−752.
(6) Rivers, T. J. H.; Terry, W.; Schmidt, Christine E. *Adv. Funct. Mater.* **2002**, *12*, 33−37.
(7) Wong, J. Y.; Langer, R.; Ingber, D. E. *Proc. Natl. Acad. Sci. U.S.A.* **1994**, *91*, 3201−3204.
(8) Schmidt, C. E.; Shastri, V. R.; Vacanti, J. P.; Langer, R. *Proc. Natl. Acad. Sci. U.S.A.* **1997**, *94*, 8948−8953.
(9) Wang, Z.; Roberge, C.; Dao, L. H.; Wan, Y.; Shi, G.; Rouabhia, M.; Guidoin, R.; Zhang, Z. *J. Biomed. Mater. Res.* **2004**, *70*, 28−38.
(10) Richardson-Burns, S. M.; Hendricks, J. L.; Foster, B.; Povlich, L. K.; Kim, D. H.; Martin, D. C. *Biomaterials* **2007**, *28*, 1539−1552.

(11) Asplund, M.; Thaning, E.; Lundberg, J.; Sandberg-Nordqvist, A. C.; Kostyszyn, B.; Inganas, O.; von Holst, H. *Biomed. Mater.* **2009**, *4*, 045009.
(12) Huang, L.; Zhuang, X.; Hu, J.; Lang, L.; Zhang, P.; Wang, Y.; Chen, X.; Wei, Y.; Jing, X. *Biomacromolecules* **2008**, *9*, 850−858.
(13) Guimard, N. K. E.; Sessler, J. L.; Schmidt, C. E. *Macromolecules* **2009**, *42*, 502−511.
(14) Liu, Y. D.; Hu, J.; Zhuang, X. L.; Zhang, P. B. A.; Chen, X. S.; Wei, Y.; Wang, X. H. *Macromol. Biosci.* **2011**, *11*, 806−813.
(15) Durgam, H.; Sapp, S.; Deister, C.; Khaing, Z.; Chang, E.; Luebben, S.; Schmidt, C. E. *J. Biomater. Sci. Polym. Ed.* **2010**, *21*, 1265−1282.
(16) Runge, M. B.; Dadsetan, M.; Baltrusaitis, J.; Knight, A. M.; Ruesink, T.; Lazcano, E. A.; Lu, L. C.; Windebank, A. J.; Yaszemski, M. J. *Biomaterials* **2010**, *31*, 5916−5926.
(17) Heisey, C. L.; Wightman, J. P.; Pittman, E. H.; Kuhn, H. H. *Textile Res. J.* **1993**, *63*, 247−256.
(18) Shi, G.; Rouabhia, M.; Wang, Z.; Dao, L. H.; Zhang, Z. *Biomaterials* **2004**, *25*, 2477−2488.
(19) Lee, J. Y.; Bashur, C. A.; Goldstein, A. S.; Schmidt, C. E. *Biomaterials* **2009**, *30*, 4325−4335.
(20) Guo, B. L.; Sun, Y.; Finne-Wistrand, A.; Mustafa, K.; Albertsson, A. C. *Acta Biomater.* **2012**, *8*, 144−153.
(21) Tessier, D.; Dao, L. H.; Zhang, Z.; King, M. W.; Guidoin, R. *J. Biomater. Sci. Polym. Ed.* **2000**, *11*, 87−99.
(22) Kim, H. S.; Hobbs, H. L.; Wang, L.; Rutten, M. J.; Wamser, C. C. *Synth. Met.* **2009**, *159*, 1313−1318.
(23) Muller, D.; Rambo, C. R.; Recouvreux, D. O. S.; Porto, L. M.; Barra, G. M. O. *Synth. Met.* **2011**, *161*, 106−111.
(24) Kelly, F. M.; Johnston, J. H.; Borrmann, T.; Richardson, M. J. *J. Nanosci. Nanotechnol.* **2008**, *8*, 1965−1972.
(25) Kaynak, A.; Wang, L. J.; Hurren, C.; Wang, X. G. *Fiber Polym.* **2002**, *3*, 24−30.
(26) Wang, Y.; Kim, H. J.; Vunjak-Novakovic, G.; Kaplan, D. L. *Biomaterials* **2006**, *27*, 6064−6082.
(27) Zhou, C. Z.; Confalonieri, F.; Jacquet, M.; Perasso, R.; Li, Z. G.; Janin, J. *Proteins* **2001**, *44*, 119−122.
(28) Altman, G. H.; Diaz, F.; Jakuba, C.; Calabro, T.; Horan, R. L.; Chen, J.; Lu, H.; Richmond, J.; Kaplan, D. L. *Biomaterials* **2003**, *24*, 401−416.
(29) Xia, Y.; Yun, L. *Compos. Sci. Technol.* **2008**, *68*, 1471−1479.
(30) Boschi, A.; Arosio, C.; Cucchi, I.; Bertini, F.; Catellani, M.; Freddi, G. *Fiber Polym.* **2008**, *9*, 698−707.
(31) Aznar-Cervantes, S.; Roca, M. I.; Martinez, J. G.; Meseguer-Olmo, L.; Cenis, J. L.; Moraleda, J. M.; Otero, T. F. *Bioelectrochem.* **2012**, *85*, 36−43.
(32) Murphy, A. R.; St John, P.; Kaplan, D. L. *Biomaterials* **2008**, *29*, 2829−2838.
(33) Huang, Z. Y.; Wang, P. C.; MacDiarmid, A. G.; Xia, Y. N.; Whitesides, G. *Langmuir* **1997**, *13*, 6480−6484.
(34) Green, R. A.; Hassarati, R. T.; Bouchinet, L.; Lee, C. S.; Cheong, G. L. M.; Yu, J. F.; Dodds, C. W.; Suaning, G. J.; Poole-Warren, L. A.; Lovell, N. H. *Biomaterials* **2012**, *33*, 5875−5886.
(35) Lawrence, B. D.; Wharram, S.; Kluge, J. A.; Leisk, G. G.; Omenetto, F. G.; Rosenblatt, M. I.; Kaplan, D. L. *Macromol. Biosci.* **2010**, *10*, 393−403.
(36) Lu, S.; Wang, X.; Lu, Q.; Zhang, X.; Kluge, J. A.; Uppal, N.; Omenetto, F.; Kaplan, D. L. *Biomacromolecules* **2010**, *11*, 143−150.
(37) Sadki, S.; Schottland, P.; Brodie, N.; Sabouraud, G. *Chem. Soc. Rev.* **2000**, *29*, 283−293.
(38) Otero, T. F.; Cascales, J. J. L.; Arenas, G. V. *Mater. Sci. Eng., C* **2007**, *27*, 18−22.
(39) Thieblemont, J. C.; Gabelle, J. L.; Planche, M. F. *Synth. Met.* **1994**, *66*, 243−247.
(40) Rapi, S.; Bocchi, V.; Gardini, G. P. *Synth. Met.* **1988**, *24*, 217−221.
(41) Malinauskas, A. *Polymer* **2001**, *42*, 3957−3972.
(42) Warren, L. F.; Walker, J. A.; Anderson, D. P.; Rhodes, C. G.; Buckley, L. J. *J. Electrochem. Soc.* **1989**, *136*, 2286−2295.
(43) Kuhn, H. H.; Child, A. D.; Kimbrell, W. C. *Synth. Met.* **1995**, *71*, 2139−2142.
(44) Hakansson, E.; Lin, T.; Wang, H. X.; Kaynak, A. *Synth. Met.* **2006**, *156*, 1194−1202.
(45) Saurin, M.; Armes, S. P. *J. Appl. Polym. Sci.* **1995**, *56*, 41−50.
(46) Yuan, Y. J.; Adeloju, S. B.; Wallace, G. G. *Eur. Polym. J.* **1999**, *35*, 1761−1172.
(47) Mccormac, T.; Breen, W.; Mcgee, A.; Cassidy, J. F.; Lyons, M. E. G. *Electroanal.* **1995**, *7*, 287−289.
(48) Cui, X.; Martin, D. C. *Sens. Actuators, B* **2003**, *89*, 92−102.
(49) Yang, J.; Martin, D. C. *Sens. Actuators, A* **2004**, *113*, 204−211.
(50) Horan, R. L.; Antle, K.; Collette, A. L.; Wang, Y.; Huang, J.; Moreau, J. E.; Volloch, V.; Kaplan, D. L.; Altman, G. H. *Biomaterials* **2005**, *26*, 3385−3393.
(51) Kotwal, A.; Schmidt, C. E. *Biomaterials* **2001**, *22*, 1055−1064.
(52) Svennersten, K.; Bolin, M. H.; Jager, E. W.; Berggren, M.; Richter-Dahlfors, A. *Biomaterials* **2009**, *30*, 6257−6264.
(53) Molino, P. J.; Higgins, M. J.; Innis, P. C.; Kapsa, R. M.; Wallace, G. G. *Langmuir* **2012**, *28*, 8433−8445.
(54) Wan, A. M.; Schur, R. M.; Ober, C. K.; Fischbach, C.; Gourdon, D.; Malliaras, G. G. *Adv. Mater.* **2012**, *24*, 2501−2505.
(55) Beh, W. S.; Kim, I. T.; Qin, D.; Xia, Y. N.; Whitesides, G. M. *Adv. Mater.* **1999**, *11*, 1038−1041.
(56) Guo, T.-F.; Chang, S.-C.; Pyo, S.; Yang, Y. *Langmuir* **2002**, *18*, 8142−8147.
(57) Kim, D. H.; Viventi, J.; Amsden, J. J.; Xiao, J.; Vigeland, L.; Kim, Y. S.; Blanco, J. A.; Panilaitis, B.; Frechette, E. S.; Contreras, D.; Kaplan, D. L.; Omenetto, F. G.; Huang, Y.; Hwang, K. C.; Zakin, M. R.; Litt, B.; Rogers, J. A. *Nat. Mater.* **2010**, *9*, 511−517.